8144–8152 *Nucleic Acids Research, 2016, Vol. 44, No. 17* *Published online 1 June 2016*
doi: 10.1093/nar/gkw496

Heat shock represses rRNA synthesis by inactivation of TIF-IA and lncRNA-dependent changes in nucleosome positioning

Zhongliang Zhao, Marcel A. Dammert, Sven Hoppe, Holger Bierhoff and Ingrid Grummt*

Division of Molecular Biology of the Cell II, German Cancer Research Center, DKFZ-ZMBH Alliance, D-69120 Heidelberg, Germany

Received February 24, 2016; Revised May 17, 2016; Accepted May 23, 2016

ABSTRACT

Attenuation of ribosome biogenesis in suboptimal growth environments is crucial for cellular homeostasis and genetic integrity. Here, we show that shutdown of rRNA synthesis in response to elevated temperature is brought about by mechanisms that target both the RNA polymerase I (Pol I) transcription machinery and the epigenetic signature of the rDNA promoter. Upon heat shock, the basal transcription factor TIF-IA is inactivated by inhibition of CK2-dependent phosphorylations at Ser170/172. Attenuation of pre-rRNA synthesis in response to heat stress is accompanied by upregulation of *PAPAS,* a long non-coding RNA (lncRNA) that is transcribed in antisense orientation to pre-rRNA. *PAPAS* interacts with CHD4, the adenosine triphosphatase subunit of NuRD, leading to deacetylation of histones and movement of the promoter-bound nucleosome into a position that is refractory to transcription initiation. The results exemplify how stress-induced inactivation of TIF-IA and lncRNA-dependent changes of chromatin structure ensure repression of rRNA synthesis in response to thermo-stress.

INTRODUCTION

All organisms sense and respond to conditions that stress their homeostasis. To ensure cell survival under stress conditions, response pathways have evolved that alter cell metabolism and maintain homeostasis in suboptimal growth environments (1). Heat shock, a moderate increase in temperature, damages cellular structures and induces an adaptive program viewed as a prototypic stress response. The heat shock response includes upregulation of genes encoding cytoprotective proteins, whereas transcription of the majority of genes is repressed (2). One of the strategies which cells use to preserve energy homeostasis under stress conditions is attenuation of ribosome biosynthesis. As rRNA synthesis is the most energy-consuming cellular process, almost all signaling pathways that affect cell growth and proliferation directly regulate rRNA synthesis, their downstream effectors converging at the RNA polymerase I (Pol I) transcription machinery (3). Upon heat shock, nucleoli disassemble and granular depositions composed of incorrectly processed ribosomal RNAs and aggregated ribosomal proteins become visible (4–9). Furthermore, many nucleolar proteins relocate to the cytoplasm, whereas other proteins are sequestered and immobilized in the nucleolus during the heat response (10).

Previous studies have established that TIF-IA, the mammalian homolog of yeast Rrn3p (11,12), plays a key role in regulation of rRNA synthesis in response to external signals. TIF-IA interacts with both Pol I and the TBP-containing factor TIF-IB/SL1, thereby bridging these two multi-subunit complexes. The activity of TIF-IA is regulated by a complex pattern of activating and inactivating phosphorylations, which ultimately fine-tune the transcriptional output (13–16). In addition to differential phosphorylation patterns in response to specific signaling pathways, phosphorylation and dephosphorylation of TIF-IA at two serine residues, Ser170/172, occurs during each round of transcription. Phosphorylation of Ser170/172 by protein kinase CK2 triggers dissociation of TIF-IA from Pol I after transcription initiation and promoter escape, while dephosphorylation by FCP1 promotes re-association of TIF-IA with Pol I, thus facilitating re-initiation and sustaining multiple rounds of transcription (17).

Recent evidence suggests that long non-coding RNAs (lncRNAs) are key players in the cellular stress response (18,19). In a previous study we have shown that a lncRNA that is transcribed in antisense orientation to pre-rRNA, termed *PAPAS* (‘promoter and pre-rRNA antisense’), is upregulated in density-arrested and serum-deprived cells (20). *PAPAS* interacts with the histone methyltransferase

*To whom correspondence should be addressed. Tel: +49 6221 423 423; Fax: +49 6221 423 467; Email: i.grummt@dkfz.de
Present address: Holger Bierhoff, Department of Genetics, Faculty of Biology and Pharmacy, Friedrich Schiller University Jena, Philosophenweg 12, 07743 Jena, Germany.

Suv4-20h2, thereby targeting Suv4-20h2 to rDNA. Suv4-20h2 trimethylates histone H4 at lysine 20 (H4K20me3), which in turn triggers chromatin compaction and augments transcriptional repression upon growth arrest. In the present study we show that *PAPAS* is also upregulated upon heat shock. Unlike growth arrest, however, *PAPAS* impacts rDNA transcription by guiding the NuRD (Nucleosome Remodeling and Deacetylase) complex to the rDNA promoter, leading to histone deacetylation and movement of the promoter-bound nucleosome into a position that is incompatible with transcription initiation. The results demonstrate that cells use two mechanisms to throttle ribosome biogenesis in response to elevated temperatures, involving inactivation of TIF-IA and *PAPAS*-dependent recruitment of NuRD to establish a transcription-refractory chromatin structure.

MATERIALS AND METHODS

Plasmids, siRNAs and antibodies

Expression plasmids and pBabe-puro retroviral vectors for FLAG- and GFP-tagged TIF-IA and for GFP-, ER- or FLAG-tagged Suv4-20h2 have been described (20). Expression plasmids for GFP-CHD4 and Nedd4-GFP were gifts from Alexander Brehm and Hiroshi Kawabe, respectively. *PAPAS*-targeting siRNAs (SilencerSelect, Life Technologies) cover sequences −78/−98 and −100/−121, CHD4 siRNAs were siGENOME SMART pools from Dharmacon (M-052142-01-0005). About 10–40 nM siRNAs were transfected into NIH3T3 cells using RNAiMAX transfection reagent (Life Technologies). Cells were harvested 36–48 h post-transfection. Antibodies against UBF, nucleolin, ERα, CHD4, MTA2 and HDAC1 were from Santa Cruz, antibodies against FLAG-epitope (M2), β-actin, β-tubulin and BrdU were from Sigma-Aldrich. Histone-specific antibodies (H3, H3K9me3, H3K4me3, H4K20me3) were from Diagenode or from Merck Millipore (acetyl-histone H4), the antibody recognizing the phosphorylated CK2 target motif (pSDXE) was from Cell Signaling Technology (CST).

Cell culture, transfection and retroviral infection

NIH3T3 and HEK293T cells were cultured in Dulbecco's modified Eagle's medium (DMEM) supplemented with 10% fetal calf serum (FCS). For heat shock, cells were transferred to pre-warmed DMEM (42°C) and incubated at 42°C for the times indicated in the figure legends. NIH3T3 cells were transfected using Lipofectamine 2000, HEK293T and Phoenix cells with the calcium phosphate precipitation method. pBabe-puro plasmids were transfected into Phoenix cells to produce retroviruses used for infection. The culture medium was collected after 36–48 h, transferred to NIH3T3 cells, and infected cells were selected with 7.5 μg/ml puromycin.

Tryptic phosphopeptide mapping

HEK293T expressing FLAG-TIF-IA were incubated in phosphate-free DMEM with 10% dialyzed FCS for 45 min before labeling with 0.5 mCi/ml [^{32}P]orthophosphate for 3 h at 37 or 42°C. Cells were lysed in 20 mM Tris–HCl [pH 7.4], 200 mM NaCl, 2 mM ethylenediaminetetraacetic acid (EDTA), 2 mM EGTA, 1% Triton X-100, 0.1% sodium dodecyl sulphate (SDS), 10 mM β-glycerophosphate, 10 mM KH2PO4, 1 mM Na3VO4 in the presence of protease inhibitors, ectopic TIF-IA was immunoprecipitated with anti-FLAG (M2) antibody, subjected to sodium dodecyl sulphate-polyacrylamide gel electrophoresis and transferred to a nitrocellulose membrane. TIF-IA was digested overnight at 37°C with trypsin (Promega, sequencing grade) and peptides were resolved on cellulose thin-layer plates as described (14).

Transcriptional analysis

RNA was reverse transcribed using M-MLV reverse transcriptase (Life Technologies) using random hexamers or sequence-specific primers (see Supplementary Table S1). *PAPAS* cDNA was synthesized with primers fused to the T7 promoter and amplified by polymerase chain reaction (PCR) using a T7 forward primer and an rDNA-specific reverse primer. Primers are listed in Supplementary Table S1. For nuclear run-on assays, cells were incubated on ice for 20 min in permeabilization buffer (50 mM Tris–HCl [pH 7.4], 5 mM $MgCl_2$, 0.5 mM EGTA, 25% glycerol, 0.15% Triton X-100, protease inhibitor cocktail), transferred to transcription buffer (50 mM Tris–HCl [pH 7.4], 25 mM KCl, 5 mM $MgCl_2$, 0.5 mM EGTA, 25% glycerol, 0.5 mM ATP/CTP/GTP, 50 μM UTP, 0.01 μCi/μl [α-^{32}P]-UTP, 80 μg/ml α-amanitin) and incubated for 20 min at 30°C. RNA was precipitated with trichloroacetic acid, collected on glass fiber filters and radioactivity was measured. Alternatively, pre-rRNA was metabolically labeled with [^{3}H]-uridine (Perkin Elmer) for 2 h and RNA was analyzed by gel electrophoresis and fluorography. To label nascent RNA, cells grown on coverslips were incubated with 2 mM 5-fluorouridine (5-FUrd) for 20 min, fixed with 1% paraformaldehyde, permeabilized with 0.5% Triton X-100, and immunostained with anti-BrdU antibody and a secondary antibody coupled to Alexa-488. Immunofluorescent pictures were recorded with a Zeiss Axiophot microscope and Nikon DXM1200 camera.

Chromatin immunoprecipitation (ChIP) assays

Chromatin immunoprecipitation (ChIP) assays were performed as described (20). Briefly, cells were cross-linked (1% formaldehyde, 10 min at room temperature) and lysed nuclei were sonicated to yield chromatin fragments of about 200–500 bp. After dilution with five volumes of ChIP-buffer (15 mM Tris–HCl [pH 8.0], 180 mM NaCl, 1.2 mM EDTA, 1.2% Triton X-100) and pre-clearing, 20 μg chromatin were incubated with 1–5 μg antibodies at 4°C overnight, immobilized on protein A/G Sepharose and washed twice in low salt buffer (20 mM Tris–HCl [pH 8.0], 150 mM NaCl, 2 mM EDTA, 0.1% SDS, 1% Triton X-100), high salt buffer (20 mM Tris–HCl [pH 8.0], 500 mM NaCl, 2 mM EDTA, 0.1% SDS, 1% Triton X-100), LiCl buffer (10 mM Tris–HCl [pH 8.0], 250 mM LiCl, 1 mM EDTA, 1% sodium deoxycholate, 1% NP-40) and TE buffer. After elution with 1% SDS/0.1 M $NaHCO_3$, chromatin was de-crosslinked at 65°C and DNA was purified on PCR purification columns (Quiagen).

Quantitative real-time PCR (qPCR) was performed using a LightCycler (Roche) and the SYBR Green detection system. The qPCR primers used to analyze precipitated DNA are included in Supplementary Table S1.

RNA and protein co-immunoprecipitation assays

To monitor protein–protein and RNA–protein interactions, cells overexpressing GFP- or F FLAG-tagged proteins were lysed in IP buffer (20 mM Tris–HCl [pH 8.0], 200 mM NaCl, 1 mM EDTA, 1 mM EGTA, 0.5% Triton X-100, protease inhibitor), cleared by centrifugation, and the supernatants were incubated for 4 h at 4°C with GFP-Trap (Chromotek) or anti-FLAG M2-agarose (Sigma-Aldrich). The immunoprecipitates were washed with IP buffer, eluted with SDS sample buffer and analyzed on immunoblots. For RNA immunoprecipitation (RIP) experiments, protein-bound RNA was eluted by digestion with proteinase K, purified with TRI Reagent and analyzed by qRT-PCR.

In vitro transcription and pull-down assays

Biotinylated RNAs were synthesized by *in vitro* transcription using the MEGAscript T7 kit (Life Technologies). Transcripts were purified with RNeasy Mini kit (QIAGEN), immobilized on streptavidin-coupled Dynabeads (Life Technologies), and incubated with lysates from HEK293T cells expressing ectopic CHD4. After washing with IP buffer, RNA-bound proteins were eluted with SDS and analyzed by western blotting.

Nucleosome positioning assay

Positions of rDNA promoter-bound nucleosomes were analyzed by LM-PCR as described (21). Briefly, cells were fixed for 10 min with 1% formaldehyde, crosslinking was quenched with 125 mM glycine for 5 min and incubated in permeabilization buffer (150 mM sucrose, 80 mM KCl, 35 mM HEPES [pH 7.4], 5 mM K_2HPO_4, 5 mM $MgCl_2$ and 0.5 mM $CaCl_2$, 0.05% L-α-lysophosphatidylcholine) for 1 min. Chromatin was digested with 50 units/ml MNase (New England Biolabs) in 150 mM sucrose, 50 mM NaCl, 50 mM Tris–HCl [pH 7.4] and 2 mM $CaCl_2$ for 20 min at room temperature. After incubation for 6 h at 65°C, DNA was purified and mononucleosome-sized fragments were recovered from 2% agarose gels with QIAquick Gel Extraction Kit (QIAGEN). DNA ends were repaired, phosphorylated with Quick Blunting Kit (New England Biolabs) and ligated to annealed linker oligonucleotides. DNA was amplified by PCR using a linker-specific primer and a ^{32}P-labeled rDNA-specific primer (−63/−36 rev). PCR products were analyzed on denaturating urea-polyacrylamide gels.

Statistical analysis

Statistical data are shown as mean values from the number of biological replicates as indicated in the figure legends with error bars denoting standard deviations (SD). Comparison between two groups was performed using a paired two-tailed Student's *t*-test, *P*-values $^{*}P < 0.05$, $^{**}P < 0.01$, $^{***}P < 0.001$.

RESULTS

TIF-IA is inactivated upon heat shock

To monitor nucleolar transcription in normal and heat shock conditions, NIH3T3 cells were pulse-labeled with 5-fluorouridine (5-FUrd) allowing visualization of nascent RNA by staining with anti-BrdU antibody. As pre-rRNA synthesis constitutes the major cellular transcriptional activity, the majority of 5-FUrd label localized in nucleoli in normal growth conditions. Nucleolar staining was abolished if cells were cultured for 2 h at 42°C, demonstrating that rDNA transcription was repressed at elevated temperatures (Figure 1A). Shut-down of nucleolar transcription in heat-shocked cells was confirmed by pulse-labeling of pre-rRNA with [^{3}H]-uridine (Supplementary Figure S1A). Time-dependent decrease of Pol I transcription was also observed in run-on assays, which showed that α-amanitin-resistant incorporation of ^{32}P-UTP into permeabilized cells was markedly reduced at 42°C (Figure 1B). In contrast to nutritional or ribotoxic stress, which leads to transition of basal Pol I transcription factors into the cytoplasm or nucleoplasm (14,15), heat shock did not displace TIF-IA and UBF from nucleoli (Supplementary Figure S1B) and did not affect promoter occupancy of UBF and TIF-IB/SL1 (Figure 1C). However, binding of Pol I and TIF-IA to rDNA was markedly compromised (Figure 1C and Supplementary Figure S1C), indicating that recruitment of the initiation-competent form of Pol I to the pre-initiation complex, consisting of UBF and TIF-IB/SL1, was impaired.

Given that Pol I is recruited to rDNA by interaction of TIF-IA with promoter-bound TIF-IB/SL1, we hypothesized that elevated temperature might trigger a mechanism that inactivates TIF-IA, which in turn would compromise Pol I binding to the rDNA promoter. TIF-IA is phosphorylated at multiple sites by a variety of protein kinases, phosphorylation at specific sites affecting TIF-IA activity (13–17). To examine whether the phosphorylation pattern of TIF-IA is altered upon heat shock, HEK293T cells overexpressing FLAG-tagged TIF-IA were metabolically labeled with [^{32}P]orthophosphate and immunopurified TIF-IA was subjected to two-dimensional tryptic phosphopeptide mapping. The pattern and intensity of most TIF-IA phosphopeptides were similar in control and stressed cells, except that the lowermost spot was markedly decreased upon exposure to 42°C (Figure 1D, encircled spot). Previous analysis of TIF-IA phosphorylation has revealed that this spot comprises two serine residues, Ser170/172, which are phosphorylated by CK2 (17). Phosphorylation of TIF-IA at Ser170/172 leads to dissociation of TIF-IA from Pol I, which is required for switching from the initiation into the elongation phase (17). Dephosphorylation of Ser170/172 by FCP1, on the other hand, facilitates the re-association of TIF-IA with Pol I, which promotes transcription initiation. Therefore cyclic phosphorylation/dephosphorylation of Ser170/172 is indispensable for multiple rounds of Pol I transcription. Decreased CK2-dependent phosphorylation of TIF-IA upon heat stress was validated on western blots using an antibody that specifically recognizes pS-DXE, a phosphorylated CK2 peptide motif (Figure 1E). Moreover, in accord with a previous study showing that

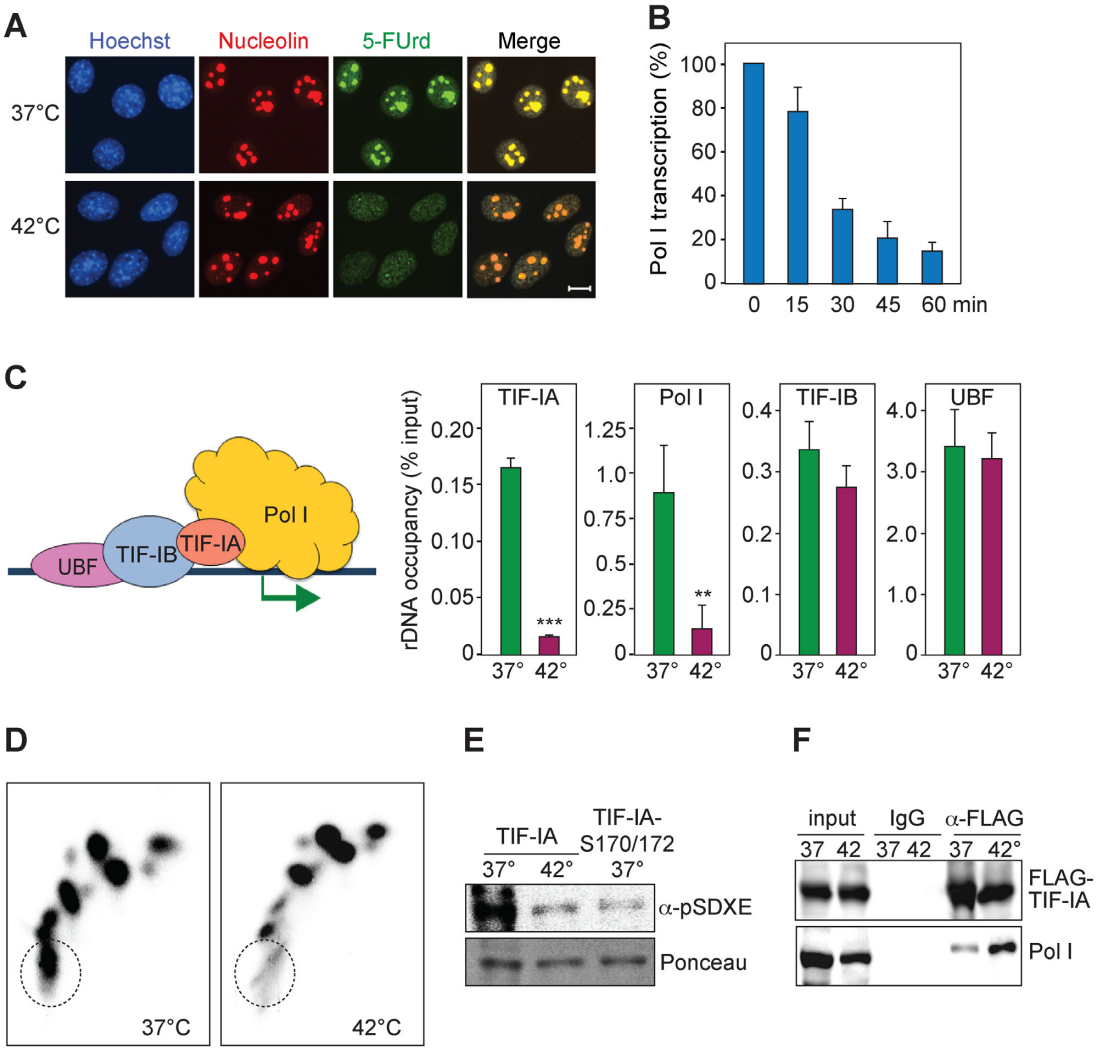

Figure 1. Heat shock inhibits pre-rRNA synthesis by preventing CK2-dependent phosphorylation of TIF-IA. (**A**) Pre-rRNA synthesis is inhibited under heat shock. NIH3T3 cells cultured at 37°C or 42°C for 2 h were pulse-labeled for 20 min with 5-fluorouridine (5-FUrd) and immunostained with antibodies against BrdU and nucleolin. The right panels show a merge of both fluorescent images. Scale bar: 10 μm. (**B**) Heat-dependent decrease of Pol I transcription *invitro*. Run-on assay using L1210 cells cultured for the indicted times at 42°C. Data display α-amanitin-resistant incorporation of [^{32}P]UTP into RNA of unstressed cells (0 min) and heat-treated cells. Bars represent means ± SD from biological triplicates. (**C**) ChIP assays monitoring occupancy of TIF-IA, Pol I (RPA116), TIF-IB and UBF at the rDNA promoter (−160/−1) upon heat shock. DNA quantified by qPCR was normalized to input. Bars represent mean values ± SD from three biological replicates ($^{**}P < 0.01$, $^{***}P < 0.001$). The cartoon illustrates factors involved in Pol I transcription initiation. (**D**) Phosphorylation of TIF-IA is altered upon heat shock. HEK293T cells expressing FLAG-TIF-IA were metabolically labeled with [^{32}P]orthophosphate at 37°C or 42°C for 3 h. Immunopurified FLAG-TIF-IA was subjected to two-dimensional tryptic phosphopeptide mapping. The spot comprising phosphoserines 170 and 172 is encircled. (**E**) CK2-dependent phosphorylation of TIF-IA is decreased upon heat shock. HEK293T cells expressing FLAG-tagged TIF-IA or TIF-IA-S170/172A were incubated at the indicated temperatures for 2 h. TIF-IA was precipitated with anti-FLAG antibody and analyzed on immunoblots for TIF-IA phosphorylation at serine 170/172 using an antibody raised against a phosphorylated CK2 substrate-peptide (pSDXE). Ponceau S staining below confirms equal loading of TIF-IA. (**F**) Increased association of TIF-IA with Pol I upon heat shock. FLAG-TIF-IA was immunoprecipitated from normal or heat-shocked HEK293T cells. FLAG-TIF-IA and co-precipitated Pol I (RPA116) were monitored on immunoblots.

CK2 is sequestered at the nuclear matrix in response to heat shock (22), phosphorylation of other cellular proteins was also reduced at 42°C (Supplementary Figure S1D). Significantly, the association of TIF-IA with Pol I was considerably stronger under elevated temperature (Figure 1F), underscoring that phosphorylation by CK2 weakens the interaction of TIF-IA with Pol I (17). Together these results demonstrate that hypophosphorylation of Ser170/172 induced by heat stress attenuates rDNA transcription by preventing CK2-dependent dissociation of TIF-IA from Pol I.

Suv4-20h2 is degraded at elevated temperature

Attenuation of Pol I transcription in growth-arrested cells has been shown to be reinforced by upregulation of a nucleolar lncRNA, termed *PAPAS*, which targets the histone methyltransferase Suv4-20h2 to rDNA and induces H4K20me3-dependent chromatin compaction (20). To examine whether *PAPAS* contributes to repression of Pol I transcription upon heat shock, we compared *PAPAS* levels in normal, serum-deprived and heat-shocked cells. In parallel, we monitored two heat-induced nucleolar lncRNAs,

IGS_{16}RNA and IGS_{22}RNA, which have been shown to sequester Hsp70 and other proteins to the intergenic spacer (IGS) separating rRNA genes (6,10). Both IGS_{16}RNA and *PAPAS* were upregulated in cells exposed to 42°C, the increase in *PAPAS* levels being more pronounced upon heat shock than upon serum deprivation (Figure 2A; Supplementary Figure S2A and B).

As upregulation of *PAPAS* in response to growth arrest recruits Suv4-20h2 to rDNA and trimethylates histone H4K20 (20), we expected that heat-induced elevation of *PAPAS* would also enhance H4K20 trimethylation. To test this, we monitored the level of H4K20me3 and other histone modifications of growing, serum-deprived and heat-shocked cells by ChIP. While there was no significant change of H3K9me3 and H3K4me3 occupancy at the rDNA promoter, acetylation of histone H4 (H4ac) was decreased both under serum deprivation and at elevated temperature (Figure 2B). However, while H4K20me3 occupancy at rDNA was 3-fold upregulated in growth-arrested cells, no significant change of H4K20me3 was observed in heat-shocked cells, indicating that upregulation of *PAPAS* does not necessarily lead to increased H4K20me3 levels. Notably, Suv4-20h2 occupancy at rDNA and global trimethylation of H4K20 were markedly decreased upon thermo-stress (Figure 2B and Supplementary Figure S2C), suggesting that compromised trimethylation of H4K20 upon heat-stress is not restricted to rDNA but may transiently regulate many other genes as well. In accord with a global decrease in H4K20me3, a strong decrease in cellular Suv4-20h2 was observed at 42°C. The decrease in Suv4-20h2 was prevented if cells were treated with the proteasome inhibitor MG132, suggesting that heat shock triggers proteasomal degradation of Suv4-20h2 (Figure 2C). In support of this notion, heat-induced loss of Suv4-20h2 was accompanied by poly-ubiquitination of Suv4-20h2 (Figure 2D). Immunoprecipitation of ubiquitinated proteins from control and heat shocked cells confirmed the appearance of more slowly moving ubiquitinated forms of Suv4-20h2 upon exposure to elevated temperature (Figure 2E).

Regarding the mechanism underlying heat-induced proteasomal degradation of Suv4-20h2, we hypothesized that the E3-ubiquitin ligase Nedd4, which targets numerous proteins in response to elevated temperature (23), may ubiquitinate Suv4-20h2. Indeed, co-immunoprecipitation experiments showed that Nedd4 interacts with Suv4-20h2, the interaction between both proteins being increased upon heat shock (Figure 2F). Moreover, while in normal conditions the great majority of Nedd4 was present in the cytoplasmic fraction, a significant fraction of Nedd4 was localized in nuclei of heat-shocked cells, nuclear translocation of Nedd4 correlating with depletion of Suv4-20h2 (Figure 2G). To provide further evidence that Nedd4 regulates Suv4-20h2 stability in response to heat stress, we monitored Suv4-20h2 levels in wild-type and *Nedd4-1*$^{-/-}$ MEFs (24). Similar to NIH3T3 cells, wild-type MEFs exhibited a strong decrease in Suv4-20h2 levels when shifted to 42°C, whereas in *Nedd4-1*$^{-/-}$ MEFs Suv4-20h2 levels were much less affected (Figure 2H). These results suggest that heat shock triggers Nedd4-dependent ubiquitination and proteasomal degradation of Suv4-20h2, thus preventing *PAPAS*-induced H4K20 trimethylation.

PAPAS recruits the chromatin remodeling complex NuRD to rDNA

As heat-induced upregulation of *PAPAS* did not lead to recruitment of Suv4-20h2 and H4K20me3-dependent chromatin compaction but correlated with deacetylation of histone H4, we hypothesized that changes in nucleosome structure might reinforce attenuation of rDNA transcription in response to heat stress. Previous studies have shown that the NuRD (Nucleosome Remodeling and Deacetylation) complex, which integrates adenosine triphosphate (ATP)-dependent chromatin remodeling and histone deacetylation activities, shifts the promoter-bound nucleosome into the transcriptional 'off' position, thereby preventing transcription initiation (25). To examine whether heat stress would affect rDNA occupancy of NuRD, we monitored the association of NuRD with the rDNA promoter in normal, serum-deprived and heat-stressed cells by ChIP. At elevated temperature, but not upon serum starvation, rDNA occupancy of the ATPase CHD4 was markedly increased (Figure 3A). rDNA occupancy of other subunits of the NuRD complex, e.g. HDAC1 and MTA2, was also increased, indicating that the NuRD complex rather than just the CHD4 subunit is recruited to rDNA (Supplementary Figure S3A). Heat-induced upregulation of *PAPAS* occurred with similar kinetics as the increase in rDNA occupancy of CHD4, linking *PAPAS* levels to enhanced binding of NuRD to rDNA (Figure 3B).

Recent studies have shown that *PAPAS* interacts with CHD4/NuRD and that upregulation of *PAPAS* upon hypo-osmotic stress recruits NuRD to rDNA (26). The correlation between increased *PAPAS* levels and rDNA occupancy of CHD4 under different stress conditions suggested that *PAPAS* might guide NuRD to rDNA under heat stress. In support of this view, RIP experiments revealed that significant amounts of *PAPAS* were associated with GFP-tagged CHD4 at elevated temperature. Under normal conditions, the interaction with *PAPAS* was weak and no interaction was observed with *HOTAIR*, an lncRNA used as a control (Figure 3C and Supplementary Figure S3B). Furthermore, both in normal and stressed cells there was marginal binding of CHD4 to IGS_{16} and IGS_{22} transcripts that are elevated upon heat stress, emphasizing the heat-specific association of CHD4/NuRD with *PAPAS* (Supplementary Figure S3C). To support the RIP data, we monitored binding of CHD4 to *PAPAS* also in pull-down experiments. After incubation of immobilized RNAs with lysates from HEK293T cells expressing GFP-tagged CHD4, significant amounts of GFP-CHD4 were retained by *PAPAS* (−1/−205) but not by its sense counterpart pRNA (−205/−1) or by IGS_{16}RNA, underscoring the specific interaction of CHD4 with *PAPAS* (Figure 3D).

Given that increased rDNA occupancy of CHD4/NuRD depends on *PAPAS*, depletion of *PAPAS* should prevent heat-induced recruitment of CHD4. To test this, we monitored CHD4 binding by ChIP in normal and stressed NIH3T3 cells in which *PAPAS* was depleted by siRNA. In accord with *PAPAS* recruiting CHD4/NuRD to rDNA, stress-induced elevation of CHD4 was attenuated after knockdown of *PAPAS* (Figure 3E). Moreover, heat-induced increased occupancy of HDAC1 and MTA2 was compro-

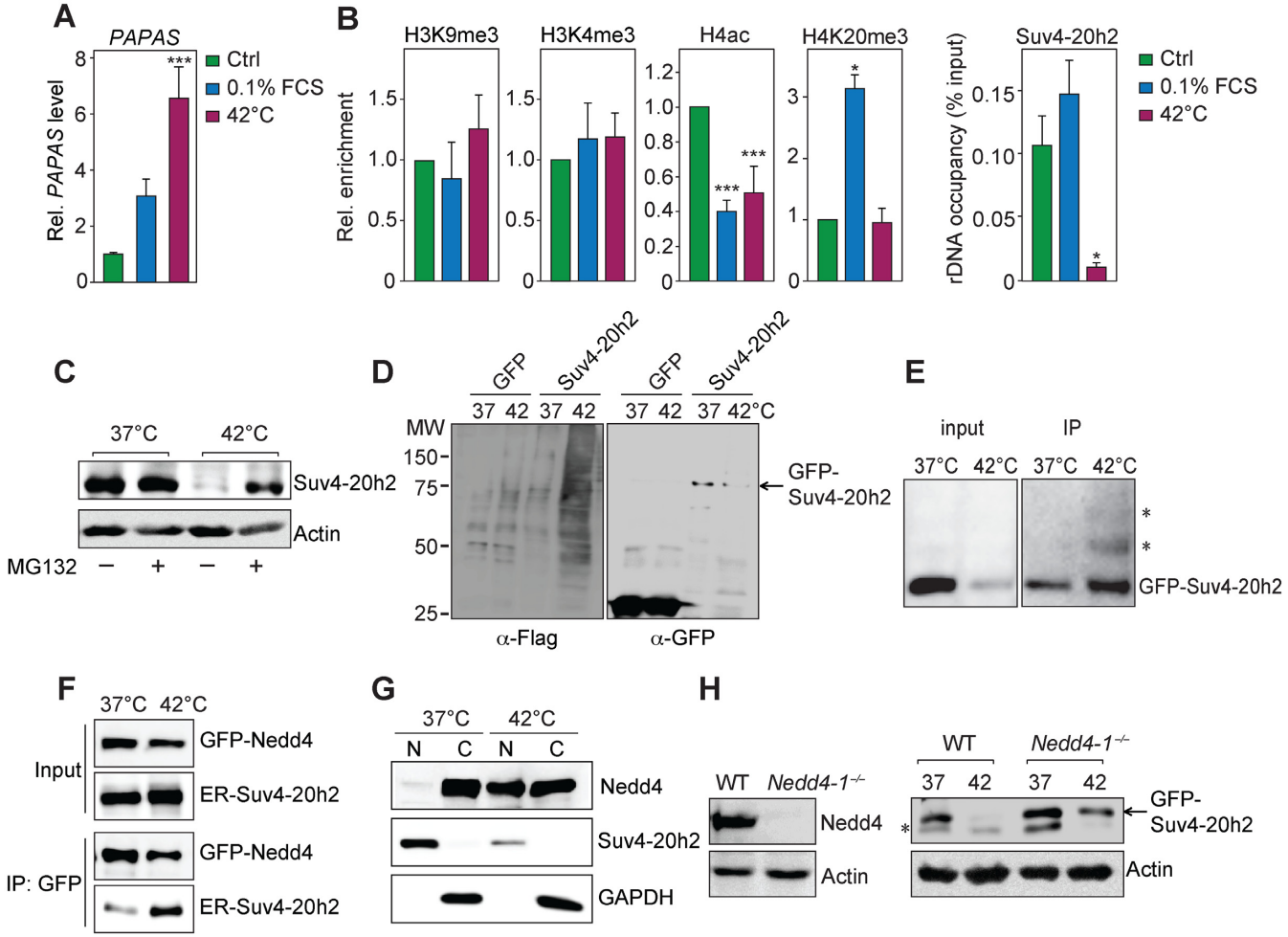

Figure 2. Heat shock leads to increased levels of *PAPAS* and degradation of Suv4-20h2. (**A**) *PAPAS* is upregulated upon growth factor deprivation and heat shock. qRT-PCR analysis of *PAPAS* normalized to 18S rRNA in NIH3T3 cells cultured in normal conditions (Ctrl), deprived of serum (0.1% FCS, 48 h) or incubated at 42°C for 3 h. Data are displayed relative to the control (Ctrl) and represent mean values ± SD from three independent experiments; $^{***}P < 0.001$. (**B**) ChIPs showing rDNA promoter occupancy of the indicated proteins in NIH3T3 cells cultured under the same conditions as in (A). Occupancy of modified histones is normalized to histone H3 and displayed relative to control conditions. Suv4-20h2 occupancy is shown relative to input. $^{*}P < 0.05$, $^{***}P < 0.001$. (**C**) Proteasomal degradation of Suv4-20h2 under elevated temperature. Western blot monitoring Suv4-20h2 and β-actin levels in NIH3T3 cells cultured at 37 or 42°C for 2 h in the absence or presence of MG132 (20 μM). (**D**) Suv4-20h2 is ubiquitinylated upon heat shock. GFP or GFP-Suv4-20h2 co-expressed with FLAG-tagged ubiquitin were immunoprecipitated after exposure of cells to 37 or 42°C for 2 h. Ubiquitinylation of Suv4-20h2 was monitored on immunoblots with anti-FLAG antibody and Suv4-20h2 with anti-GFP antibodies. (**E**) Reduced level of Suv4-20h2 upon heat shock correlates with Suv4-20h2 poly-ubiquitiation. HEK293T cells co-expressing FLAG-ubiquitin and GFP-Suv4-20h2 were cultured for 2 h at 37 or 42°C and immunoprecipitated with anti-FLAG antibody. Input and immunoprecipitated material was analyzed on western blots with anti-GFP antibodies. Asterisks indicate slower migrating Suv4-20h2-ubiquitin conjugates. (**F**) Increased association of Nedd4 with Suv4-20h2 upon heat shock. GFP-Nedd4 co-expressed with ER-Suv4-20h2 in HEK293T cells was bound to anti-GFP beads. GFP-Nedd4 and associated ER-Suv4-20h2 were analyzed by immunoblotting using anti-GFP and anti-ER antibodies. (**G**) Nedd4 translocates to the nucleus upon heat shock. NIH3T3 cells were fractionated into nuclei (N) and cytoplasm (C) and Suv4-20h2 and Nedd4 were assayed on western blots. The cytosolic marker protein GAPDH was assayed to control cell fractionation. (**H**) Heat-dependent degradation of Suv4-20h2 is brought about by Nedd4. Western blot monitoring GFP-Suv4-20h2 in normal MEFs (WT) or in Nedd4-deficient MEFs (*Nedd4-1*$^{-/-}$) grown at 37 or 42°C for 3 h. β-actin served as a loading control. The arrow marks the position of GFP-Suv4-20h2, the asterisk a non-specific band.

mised in CHD4-depleted cells (Figure 3F; Supplementary Figure S3D and E), supporting that binding of CHD4 to *PAPAS* is required for targeting NuRD to rDNA. Finally, knockdown of CHD4 increased acetylation of histone H4, the increase being more pronounced upon heat shock as compared to normal conditions (Figure 3G). This result is in accord with heat stress inducing *PAPAS*-dependent recruitment of NuRD, which deacetylates nucleosomes at the rDNA promoter and establishes a specific chromatin structure at rRNA genes that are poised for transcription activation (25).

NuRD shifts the promoter-bound nucleosome into the transcriptional 'Off' position

Active and silent rRNA genes exhibit different histone modifications and nucleosome positions. At transcriptionally active genes, the promoter-bound nucleosome extends from nucleotide −157 to −2, whereas the nucleosome at silent

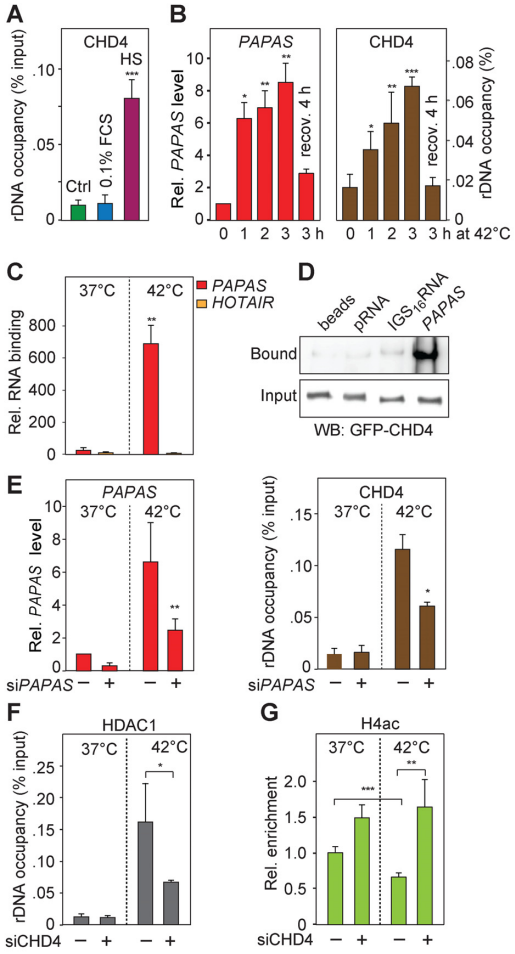

Figure 3. *PAPAS* recruits NuRD to rDNA. (**A**) Increased rDNA occupancy of CHD4 in heat-shocked cells. ChIP of CHD4 in NIH3T3 cells cultured under normal conditions (Ctrl), upon serum deprivation (0.1% FCS) or at 42°C for 3 h. Binding to the rDNA promoter relative to input is displayed. Data are means ± SD of three independent experiments, $^{***}P < 0.001$. (**B**) Increased *PAPAS* levels correlate with increased rDNA occupancy of CHD4 under heat stress. *PAPAS* levels relative to 18S rRNA (red bars) and ChIP of CHD4 (brown bars) from cells cultured for the indicated times at 42°C or cultured for 3 h at 42°C followed by 4 h recovery at 37°C (recov.). Bars represent mean values ± SD of three independent experiments; $^{*}P < 0.05$, $^{**}P < 0.01$, $^{***}P < 0.001$. (**C**) CHD4 interacts with *PAPAS* in heat-shocked cells. GFP-tagged CHD4 was immunoprecipitated from HEK293T cells cultured at 37 or 42°C for 3 h. Co-precipitated *PAPAS* and *HOTAIR* lncRNAs were monitored by qRT-PCR and normalized to RNA immunoprecipitated from GFP-expressing cells. Bars display means ± SD of three independent experiments; $^{**}P < 0.01$. (**D**) Preferential binding of CHD4 to *PAPAS*. Pull-down assay using bead-bound lncRNAs and extracts from HEK293T cells overexpressing GFP-CHD4. Captured proteins and proteins in the input were analyzed on western blots using anti-GFP antibodies. (**E**) Recruitment of CHD4 to rDNA depends on *PAPAS*. NIH3T3 cells transfected with off-target siRNA (−) or si*PAPAS* siRNA (+) were cultured at 37 or 42°C for 3 h. Knockdown of *PAPAS* was assessed by qRT-PCR (red bars); rDNA occupancy of CHD4 by ChIP (brown bars). Bars represent mean values ± SD from three independent experiments; $^{*}P < 0.05$, $^{**}P < 0.01$. (**F**) The NuRD complex is recruited to rDNA upon heat stress. ChIP showing reduced HDAC1 binding to rDNA in NIH3T3 cells transfected with off-target (−) or CHD4-targeting (+) siRNAs upon exposure to 42°C for 3 h. ChIP enrichment relative to input is shown as mean values ± SD from three independent experiments, $^{*}P < 0.05$. (**G**) ChIP of pan-acetylated histone H4 (H4ac) after CHD4 knockdown and heat stress. Treatments were the same as in (F). H4ac levels at rDNA were normalized to histone H3. Data are means ± SD of biological triplicates; $^{**}P < 0.01$, $^{***}P < 0.001$.

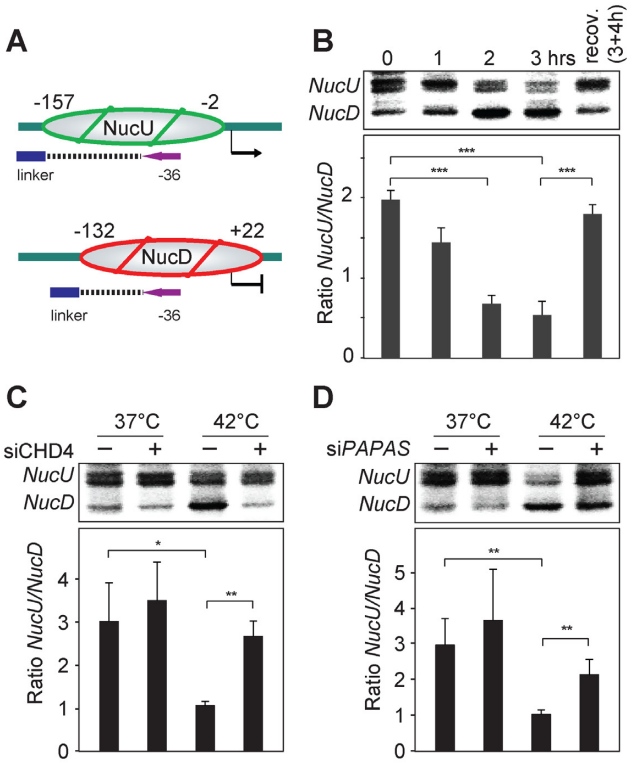

Figure 4. Stress-induced recruitment of NuRD shifts the promoter-bound nucleosome into the poised position. (**A**) Scheme depicting the two nucleosomal conformations at the rDNA promoter. The LM-PCR products corresponding to *NucU* and *NucD* are indicated. (**B**) Heat-induced changes of nucleosome positions at the rDNA promoter. LM-PCR products of mononucleosomal DNA from NIH3T3 cells cultured at 37°C (0 h) or at 42°C for the indicated times. To recover from heat stress, cells exposed to 42°C for 3 h were cultured for 4 h at 37°C (recov.). The bar diagram shows the *NucU*/*NucD* ratio determined in three independent experiments, $^{***}P < 0.001$. (**C**) Heat-induced nucleosome repositioning is compromised in CHD4-deficient cells. Nucleosome positions were assayed in NIH3T3 cells transfected with off-target (−) or CHD4-targeting (+) siRNAs and cultured at 37 or 42°C for 3 h (upper panel). The *NucU*/*NucD* ratio from three independent experiments is displayed below as means ± SD; $^{*}P < 0.05$, $^{**}P < 0.01$. (**D**) *PAPAS* is required for NuRD-dependent nucleosome movement. Nucleosome positions in NIH3T3 cells transfected with off-target siRNA (−) or si*PAPAS* siRNA (+) and cultured at 37 or 42°C for 3 h. The bar diagram shows quantification of the *NucU*/*NucD* ratio. Bars represent means ± SD from biological triplicates; $^{**}P < 0.01$.

rRNA genes is positioned 24 nucleotides further downstream (Figure 4A), placing the nucleosome into a translational position that is unfavorable for transcription complex assembly. Previous studies have shown that CHD4/NuRD is the remodeling complex that shifts the promoter-bound nucleosome into the downstream position (NucD), thereby poising transcription-permissive genes (21,25). To examine whether heat stress affects nucleosome positioning at the rDNA promoter, we analyzed nucleosome positioning in normal and heat-shocked cells by ligation-mediated PCR (LM-PCR) of crosslinked mononucleosomal DNA (Figure 4B). Visualization of radiolabeled DNA fragments after electrophoresis on sequencing gels revealed PCR fragments of different lengths, the faster migrating band representing the position of *NucD,* which marks the transcriptional 'off' position. The upper two bands with nearly identical size

correspond to the position of *NucU*, which is associated with active rRNA genes. The presence of two closely spaced *NucU* bands indicates that the position of *NucU* is more 'fuzzy' than that of *NucD*. After exposure to elevated temperature, a time-dependent repositioning of nucleosomes was observed, the majority of *NucU* moving to the *NucD* position (Figure 4B). After shifting cells back to 37°C, the original ratio of *NucU* to *NucD* was re-established, indicating that changes in nucleosome positioning are reversible. Heat-induced nucleosome movement correlated with elevated *PAPAS* levels and increased rDNA occupancy of NuRD, supporting that *PAPAS* reinforces transcriptional repression by altering the chromatin structure at the rDNA promoter. To prove that changes in nucleosome positioning were brought about by NuRD, we monitored nucleosome positioning after siRNA-mediated knockdown of CHD4. In accord with CHD4/NuRD shifting *NucU* to the *NucD* position, no increase in *NucD* was observed if CHD4-deficient cells were exposed to elevated temperature (Figure 4C). A similar attenuation of nucleosome movement was observed upon knockdown of *PAPAS*, underscoring the pivotal role of *PAPAS* in stress-dependent nucleosome remodeling (Figure 4D). Together, these results demonstrate that in heat-stressed cells increased levels of *PAPAS* trigger recruitment of NuRD, which establishes a nucleosomal architecture that prevents transcription initiation.

DISCUSSION

The nucleolar transcription machinery is the key convergence point that collects and integrates a vast array of information from cellular signaling cascades to regulate ribosome production (3,27). Almost all signaling pathways that affect cell growth and proliferation regulate ribosome biogenesis by modulating the activity of transcription factors required for rRNA synthesis. Here we show that attenuation of rDNA transcription at elevated temperature is brought about by inactivation of TIF-IA, the basal factor that mediates the interaction of Pol I with the TATA binding protein-containing factor TIF-IB/SL1 (11,28). TIF-IA is phosphorylated at several sites that positively or negatively affect its activity (13–17). Phosphorylation of Ser170/172 by CK2 was reduced upon exposure to 42°C, demonstrating that cells decrease CK2-dependent essential phosphorylations to inactivate TIF-IA and throttle rDNA transcription.

In addition to inactivation of an essential component of the Pol I transcription machinery, cells use an lncRNA- and chromatin-based mechanism to reinforce transcriptional repression at elevated temperature. In accord with lncRNAs evolving as key regulators of many cellular stressors, we found that the nucleolar lncRNA *PAPAS* is upregulated upon heat stress. Elevated levels of *PAPAS* trigger CHD4/NuRD-dependent nucleosomal remodeling, leading to movement of the promoter-bound nucleosome 24 nucleotides further downstream (*NucD*). As a consequence, the relative alignment of the core promoter and the upstream control element with respect to the histone octamer surface is changed and a translational position established that does not allow the assembly of a productive transcription initiation complex (21). RNA-dependent targeting of chromatin remodeling complexes is an attractive mechanism to alter the chromatin structure at distinct genomic loci in response to external signals. For genes transcribed by RNA polymerase II (Pol II), one mechanism by which heat shock has been found to suppress gene expression is through upregulation of inhibitory RNAs, e.g. B2 or *Alu* RNAs, that block Pol II activity. Upon stress, B2 or *Alu* RNAs directly bind to the active site within Pol II, disrupting its interaction with promoter DNA and interfering with phosphorylation of the carboxy-terminal domain (29,30). Regarding rDNA transcription, thermo-stress has been shown to trigger a rapid re-organization of the nucleolus, which is regulated by a family of lncRNA molecules derived from the IGS of rDNA. Upregulation of IGS-RNAs leads to recruitment and immobilization of proteins in the nucleolus, thus facilitating some cytoprotective effects that counteract heat stress (10). In contrast to IGS-RNAs, *PAPAS* enforces repression of rDNA transcription in response to different stress conditions. In serum-deprived and density-arrested cells, upregulation of *PAPAS* compromises transcription by recruiting the histone methyltransferase Suv4-20h2, which trimethylates H4K20 and triggers chromatin compaction (20). Upon heat stress, Suv4-20h2 is degraded by the ubiquitin-proteasome pathway, allowing *PAPAS* to interact with CHD4, the ATPase subunit of the chromatin remodeling complex NuRD. After *PAPAS*-dependent targeting to rDNA, NuRD promotes deacetylation of histones and shifts the promoter-bound nucleosome into the 'off' position that is refractory to transcription initiation. A similar NuRD-dependent mechanism was found to augment transcriptional repression in response to hypotonic stress (26). Thus the mechanism underlying *PAPAS*-mediated attenuation of rDNA transcription is not restricted to heat stress but may be commonly used to inhibit ribosome biogenesis and maintain homeostasis under unfavorable growth conditions.

Several studies have highlighted the function of lncRNA in regulation of chromatin-remodeling complexes. For example, interactions of the lncRNA *SChLAP1* with SNF5 and *Myheart* with BRG1 impair the remodeling activity of SWI/SNF (31,32). Moreover, the SWI/SNF complex has been shown to interact with Satellite III (Sat III) lncRNA and to be required for the formation of nuclear stress bodies in response to heat shock (33). An important question in the chromatin remodeling field is the mode by which individual chromatin remodeling complexes are targeted to their site of action, which is key to achieve biological specificity. Because most remodelers lack sequence-specific DNA-binding motifs, the predominant view is that they are recruited by transient interactions with DNA-binding proteins that recognize specific DNA sequences. The finding that *PAPAS* interacts with CHD4 and guides NuRD to the rDNA cassette, underscores the potential of lncRNAs in targeting chromatin modifying enzymes to distinct genomic loci, extending the function of lncRNAs as genomic 'address code' for nucleosome remodeling complexes. Thus the mechanisms underlying the nucleolar stress response are complex and intertwined, demonstrating that cells use independent strategies to attenuate rDNA transcription upon different harmful conditions to preserve cellular energy homeostasis.

SUPPLEMENTARY DATA

Supplementary Data are available at NAR Online.

ACKNOWLEDGEMENTS

We thank all members of the group for helpful discussions and support. We are grateful to Alexander Brehm for the plasmid encoding GFP-CHD4 and Hiroshi Kawabe for Nedd4-GFP and *Nedd4-1*$^{-/-}$ MEFs.
Author contributions: I.G. conceived the study and guided the project. Z.Z., M.A.D., H.B. and S.H. carried out experiments and analyzed data. All authors contributed to discussions about the data and their interpretation. The manuscript was written by I.G. and H.B. All authors contributed to the manuscript review.

FUNDING

Deutsche Forschungsgemeinschaft [GR475/22-1; SFB1036]; CellNetworks Cluster of Excellence (EcTop 5); DKFZ-MOST; Baden-Württemberg Stiftung [NCRNA_025]. Funding for open access charge: Deutsche Forschungsgemeinschaft [SFB1036].
Conflict of interest statement. None declared.

REFERENCES

1. Kultz,D. (2005) Molecular and evolutionary basis of the cellular stress response. *Annu. Rev. Physiol.*, **67**, 225–257.
2. Richter,K., Haslbeck,M. and Buchner,J. (2010) The heat shock response: life on the verge of death. *Mol. Cell*, **40**, 253–266.
3. Grummt,I. (2013) The nucleolus-guardian of cellular homeostasis and genome integrity. *Chromosoma*, **122**, 487–497.
4. Bouche,G., Raynal,F., Amalric,F. and Zalta,J.P. (1981) Unusual processing of nucleolar RNA synthesized during a heat shock in CHO cells. *Mol. Biol. Rep.*, **7**, 253–258.
5. Ghoshal,K. and Jacob,S.T. (1996) Heat shock selectively inhibits ribosomal RNA gene transcription and down-regulates E1BF/Ku in mouse lymphosarcoma cells. *Biochem. J.*, **317**, 689–695.
6. Jacob,M.D., Audas,T.E., Uniacke,J., Trinkle-Mulcahy,L. and Lee,S. (2013) Environmental cues induce a long noncoding RNA-dependent remodeling of the nucleolus. *Mol. Biol. Cell*, **24**, 2943–2953.
7. Pelham,H.R. (1984) Hsp70 accelerates the recovery of nucleolar morphology after heat shock. *EMBO J.*, **3**, 3095–3100.
8. Welch,W.J. and Feramisco,J.R. (1984) Nuclear and nucleolar localization of the 72,000-dalton heat shock protein in heat-shocked mammalian cells. *J. Biol. Chem.*, **259**, 4501–4513.
9. Welch,W.J. and Suhan,J.P. (1985) Morphological study of the mammalian stress response: characterization of changes in cytoplasmic organelles, cytoskeleton, and nucleoli, and appearance of intranuclear actin filaments in rat fibroblasts after heat-shock treatment. *J. Cell Biol.*, **101**, 1198–1211.
10. Audas,T.E., Jacob,M.D. and Lee,S. (2012) Immobilization of proteins in the nucleolus by ribosomal intergenic spacer noncoding RNA. *Mol. Cell*, **45**, 147–157.
11. Schnapp,A., Pfleiderer,C., Rosenbauer,H. and Grummt,I. (1990) A growth-dependent transcription initiation factor (TIF-IA) interacting with RNA polymerase I regulates mouse ribosomal RNA synthesis. *EMBO J.*, **9**, 2857–2863.
12. Moorefield,B., Greene,E.A. and Reeder,R.H. (2000) RNA polymerase I transcription factor Rrn3 is functionally conserved between yeast and human. *Proc. Natl. Acad. Sci. U.S.A.*, **97**, 4724–4729.
13. Zhao,J., Yuan,X., Frodin,M. and Grummt,I. (2003) ERK-dependent phosphorylation of the transcription initiation factor TIF-IA is required for RNA polymerase I transcription and cell growth. *Mol. Cell*, **11**, 405–413.
14. Mayer,C., Bierhoff,H. and Grummt,I. (2005) The nucleolus as a stress sensor: JNK2 inactivates the transcription factor TIF-IA and down-regulates rRNA synthesis. *Genes Dev.*, **19**, 933–941.
15. Mayer,C., Zhao,J., Yuan,X. and Grummt,I. (2004) mTOR-dependent activation of the transcription factor TIF-IA links rRNA synthesis to nutrient availability. *Genes Dev.*, **18**, 423–434.
16. Hoppe,S., Bierhoff,H., Cado,I., Weber,A., Tiebe,M., Grummt,I. and Voit,R. (2009) AMP-activated protein kinase adapts rRNA synthesis to cellular energy supply. *Proc. Natl. Acad. Sci. U.S.A.*, **106**, 17781–17786.
17. Bierhoff,H., Dundr,M., Michels,A.A. and Grummt,I. (2008) Phosphorylation by casein kinase 2 facilitates rRNA gene transcription by promoting dissociation of TIF-IA from elongating RNA polymerase I. *Mol. Cell. Biol.*, **28**, 4988–4998.
18. Place,R.F. and Noonan,E.J. (2014) Non-coding RNAs turn up the heat: an emerging layer of novel regulators in the mammalian heat shock response. *Cell Stress Chaperones*, **19**, 159–172.
19. Audas,T.E. and Lee,S. (2016) Stressing out over long noncoding RNA. *Biochim. Biophys. Acta*, **1859**, 184–191.
20. Bierhoff,H., Dammert,M.A., Brocks,D., Dambacher,S., Schotta,G. and Grummt,I. (2014) Quiescence-induced LncRNAs trigger H4K20 trimethylation and transcriptional silencing. *Mol. Cell*, **54**, 675–682.
21. Li,J., Langst,G. and Grummt,I. (2006) NoRC-dependent nucleosome positioning silences rRNA genes. *EMBO J.*, **25**, 5735–5741.
22. Davis,A.T., Wang,H., Zhang,P. and Ahmed,K. (2002) Heat shock mediated modulation of protein kinase CK2 in the nuclear matrix. *J. Cell. Biochem.*, **85**, 583–591.
23. Fang,N.N., Chan,G.T., Zhu,M., Comyn,S.A., Persaud,A., Deshaies,R.J., Rotin,D., Gsponer,J. and Mayor,T. (2014) Rsp5/Nedd4 is the main ubiquitin ligase that targets cytosolic misfolded proteins following heat stress. *Nat. Cell Biol.*, **16**, 1227–1237.
24. Kawabe,H., Neeb,A., Dimova,K., Young,S.M., Takeda,M., Katsurabayashi,S., Mitkovski,M., Malakhova,O.A., Zhang,D.E., Umikawa,M. *et al.* (2010). Regulation of Rap2A by the ubiquitin ligase Nedd4-1 controls neurite development . *Neuron* , **65**, 358–372.
25. Xie,W., Ling,T., Zhou,Y., Feng,W., Zhu,Q., Stunnenberg,H.G., Grummt,I. and Tao,W. (2012) The chromatin remodeling complex NuRD establishes the poised state of rRNA genes characterized by bivalent histone modifications and altered nucleosome positions. *Proc. Natl. Acad. Sci. U.S.A.*, **109**, 8161–8166.
26. Zhao,Z., Dammert,M.A., Grummt,I. and Bierhoff,H. (2016) lncRNA-induced nucleosome repositioning reinforces transcriptional repression of rRNA genes upon hypotonic stress. *Cell Rep.*, **14**, 1876–1882.
27. Boulon,S., Westman,B.J., Hutten,S., Boisvert,F.M. and Lamond,A.I. (2010) The nucleolus under stress. *Mol. Cell*, **40**, 216–227.
28. Yuan,X., Zhao,J., Zentgraf,H., Hoffmann-Rohrer,U. and Grummt,I. (2002) Multiple interactions between RNA polymerase I, TIF-IA and TAF(I) subunits regulate preinitiation complex assembly at the ribosomal gene promoter. *EMBO Rep.*, **3**, 1082–1087.
29. Mariner,P.D., Walters,R.D., Espinoza,C.A., Drullinger,L.F., Wagner,S.D., Kugel,J.F. and Goodrich,J.A. (2008) Human Alu RNA is a modular transacting repressor of mRNA transcription during heat shock. *Mol. Cell*, **29**, 499–509.
30. Yakovchuk,P., Goodrich,J.A. and Kugel,J.F. (2009) B2 RNA and Alu RNA repress transcription by disrupting contacts between RNA polymerase II and promoter DNA within assembled complexes. *Proc. Natl. Acad. Sci. U.S.A.*, **106**, 5569–5574.
31. Prensner,J.R., Iyer,M.K., Sahu,A., Asangani,I.A., Cao,Q., Patel,L., Vergara,I.A., Davicioni,E., Erho,N., Ghadessi,M. *et al.* (2013) The long noncoding RNA SChLAP1 promotes aggressive prostate cancer and antagonizes the SWI/SNF complex. *Nat. Genet.*, **45**, 1392–1398.
32. Han,P., Li,W., Lin,C.H., Yang,J., Shang,C., Nurnberg,S.T., Jin,K.K., Xu,W., Lin,C.Y., Lin,C.J. *et al.* (2014) A long noncoding RNA protects the heart from pathological hypertrophy. *Nature*, **514**, 102–106.
33. Kawaguchi,T., Tanigawa,A., Naganuma,T., Ohkawa,Y., Souquere,S., Pierron,G. and Hirose,T. (2015) SWI/SNF chromatin-remodeling complexes function in noncoding RNA-dependent assembly of nuclear bodies. *Proc. Natl. Acad. Sci. U.S.A.*, **112**, 4304–4309.